Assessing the climate change impact on hydrological response in the Gorganrood River Basin, Iran

Hamed Rouhani and Marayam Sadat Jafarzadeh

ABSTRACT

A general circulation model (GCM) and hydrological model SWAT (Soil and Water Assessment Tool) under forcing from A1B, B1, and A2 emission scenarios by 2030 were used to assess the implications of climate change on water balance of the Gorganrood River Basin (GRB). The results of MPEH5C models and multi-scenarios indicated that monthly precipitation generally decreases while temperature increases in various parts of the basin with the magnitude of the changes in terms of different stations and scenarios. Accordingly, seasonal ET will decrease throughout the GRB over the 2020s in all seasons except in summer, where a slight increase is projected for A1B and A2 scenarios. At annual scale, average quick flow and average low flow under the B1, A1B, and A2 scenarios are projected to decrease by 7.3 to 12.0% from the historical levels. Over the ensembles of climate change scenarios, the simulations project average autumn total flow declines of ~10% and an overall range of 6.9 to 13.2%. In summer, the components of flow at the studied basin are expected to increase under A2 and A1B scenarios but will slightly decrease under B1 scenario. The study result addresses a likelihood of inevitable future climate change.

Key words | climate change, emission scenario, SWAT, water balance

Hamed Rouhani (corresponding author)
Department of Range and Watershed Management, College of Agriculture Science and Natural Resource,
Gonbad-e-Kavous University,
Golestan,
Iran
E-mail: *rouhani.hamed@gonbad.ac.ir*

Marayam Sadat Jafarzadeh
Department of Range and Watershed Management,
Lorestan University,
Lorestan,
Iran

INTRODUCTION

Weather, climate variability, and climate change are important considerations in water resources-related investigations, such as urban water policy, environmental quality assessments (Delgado *et al.* 2011), distribution and productivity of terrestrial vegetation (Hatfield *et al.* 2011), land resources management (Nearing *et al.* 2004), ecology (Lal *et al.* 2011), and sediment yield (Shrestha *et al.* 2013). In this context, concern has grown in recent years over the issue of global climate change in which increased greenhouse gas emissions lead to changes in the distribution of water resources over many regions. The global and regional hydrological cycles have been greatly influenced by climate change in the past century (Scanlon *et al.* 2007; Schneeberger *et al.* 2015; Zang *et al.* 2015) and the availability and distribution of freshwater resources will be greatly affected by climate change thus having the potential to impose additional water stress (Parry *et al.* 2007). It has also been recognized that climate change is foreseen to increase water stress in some parts of the world and increase flood risk in others (Arnell 2004), along with a decline in water quality. This will affect the terrestrial water cycle and human livelihoods in the future (Srikanthan & McMahon 2001; Xu & Singh 2004).

This emphasizes the importance to assess the motivation for climate change considerations in the adaptive management of water resources. Modeling the hydrologic impacts of climate change on river basins involves two issues (e.g., Jiang *et al.* 2007): climate change and hydrologic systems response. Climate models, called general circulation models (GCMs), are used to project the potential climate

doi: 10.2166/wcc.2017.207

change for assumed future greenhouse gas emission scenarios. The long time scales and uncertainty due to global change have led analysts to develop 'scenarios' of future environmental, social, and economic changes to improve understanding among decision-makers of the potential consequences of their decisions.

The Gorganrood River Basin (GRB), located in the southern belt of the Caspian Sea, Iran, has an area of about 13,000 km^2 and includes densely populated and highly agricultural lands. The river is of great economic and environmental importance for the region. The major floods in 2001 and 2002, that caused huge damage, and the dry summers in recent years have revealed the vulnerability of water management systems to changes in the hydrological regime of the GRB. Regarding the potentially large socio-economic impacts, it has become recognized that climate-induced changes in the discharge regime of the GRB should become factored into water management. Based primarily on statistical trend analyses of observed climatology, many of these studies (Araghinejad *et al.* 2013; Jafarzadeh *et al.* 2016b; Malekian & Kazemzadeh 2016) speculated that changes in water resources have resulted from climate change, especially changes in precipitation and temperature. Seasonal climate variability and change could modify rainfall and snowfall patterns, change runoff volume and timing, increase sea levels, and change urban and agricultural water demands. An increase in temperature may result in an increase in evapotranspiration demand rate, and that, in combination with a reduction in precipitation, will severely stress the water resources in the region. On the other hand, human activities such as land use change and artificial water intake in the GRB have led to environmental degradation and water shortages (Pasandidehfard *et al.* 2014). Over the past decade, some studies have been carried out in the GRB, mainly focusing on the stream flow forecasts. Salmani *et al.* (2013) used the water balance model with a spatially semi-distributed approach to estimate daily river flow discharge of the GRB. Modaresi *et al.* (2012) examined a conditional probability distribution function to determine the quantity of the annual water yield of the GRB. The output from scenario B2 of the HadCM3 model was used to compare the basin runoff of a baseline period (1977–2006) to a future 30-year period, 2040–69. It was shown that the future runoff in Tamar station located inside the GRB, will decrease by up to 1.38% and 1.33% in return periods of 50 and 100 years, respectively, as a result of the projected increases in temperature and decrease in precipitation.

Assessing the hydrological impacts basically relies on water budget modeling and analysis of the interaction among precipitation, evapotranspiration, soil moisture, and runoff under the influences of changing climate, using climate models, downscaling techniques, and hydrological models. In recent years, there have been many studies of the temperature, precipitation (Sheikh *et al.* 2009; Jafarzadeh *et al.* 2016a, 2016b), river flow (Modaresi *et al.* 2012; Salmani *et al.* 2013) and irrigation demand and crop growth in the GRB (Ghorbani *et al.* 2013), but there have been no studies of the flows of both green and blue water. Therefore, a detailed and integrated analysis of the water resource trends is urgently needed to support water management for the entire river basin. What is lacking in these studies is the quantification of the changes in water balance terms with respect to the climate change. Also, the IPCC calls for expanded research on local impacts of climate change and finer-resolution assessments of changes in water balance.

Water balance models have been used to accurately simulate spatial and temporal patterns of green and blue water flows (e.g., Zang *et al.* 2012), forecast changes in discharges based on climate changes (e.g., Arnell 1992; Jiang *et al.* 2007), and are relatively straightforward to apply. Thus, water balance models could be an empowering tool for water resource managers to prepare for and mitigate the effects of regional climate change on their local hydrologic resources. The overall objective of this study is to undertake the effects of projected climatic changes of the GRB on individual hydrologic components at the downstream parts of the river. As the GRB is a vulnerable region due to its potential in various land use activities there are different water-based projects which are attached to the flow of Gorganrood River. The projects include existing and proposed irrigation schemes and tourism at different parts of the river. Hence, estimation of monthly and long-term runoff yield helps to identify the best and sustainable land use and management options in the area. Therefore, the output of this study can be taken as an input to plan and implement the effective land and water resources

development and management. Here, climate projections from a GCM, and three emission scenarios, and a semi-distributed hydrological model are used to assess the response of the terrestrial hydrological cycle to climate change and subsequent changes in available water resources.

MATERIALS AND METHODS

Study area and data

The basin is located in the midstream of the Gorganrood River, northeastern Iran. The Golestan Regional Water Company (GRWC) monitoring site at Gazaghly (Figure 1) was chosen as the outlet for the entire basin since it is the lowest monitoring station on the river not subject to dam influence. The total drainage area of the basin (36° 48′ ~ 37° 47′ N, 55° 01′ ~ 56° 27′ E) is about 7,072 km^2, with a length of 192.47 km for the major channel. The basin's elevation ranges between 2,889 m to approximately 30 m above sea level at the outlet. The mean elevation of the basin is 1,014 m and the mean slope of the basin is about 15%. Geographically, it is divided into two different sections, the plains and the mountains of the Alborz chain, and the direction of the mountains faces northeast and gradually decreases in height. The dominating land use class is 'grassland–shrub land' with an average of 35%. As a result of the large topographic variability, its distance from the sea, the desert areas south of Turkmenistan, and local winds, the basin contains many areas with district micro-climatic conditions that influence the land use systems. The climate of the basin is variable; the southern part has a typical mountainous climate, the central and southwestern regions have a temperate Mediterranean climate, and the northern part is semi-arid land. Annual precipitation decreases in the west to east direction, low (200 mm) to high (880 mm) and from south to north direction. Rainfall is highly seasonal, of which the spring, summer, autumn, and winter contribute 23, 15, 27, and 35% of the average annual rainfall, respectively. In the last decades, the basin has witnessed extreme events; massive floods as well as water shortages. The climate data for seven weather stations used for the model simulation were obtained from the Iranian National Meteorological Organization and the GRWC. Monthly river discharge was obtained for the site located at the basin outlet in Gazaghly station.

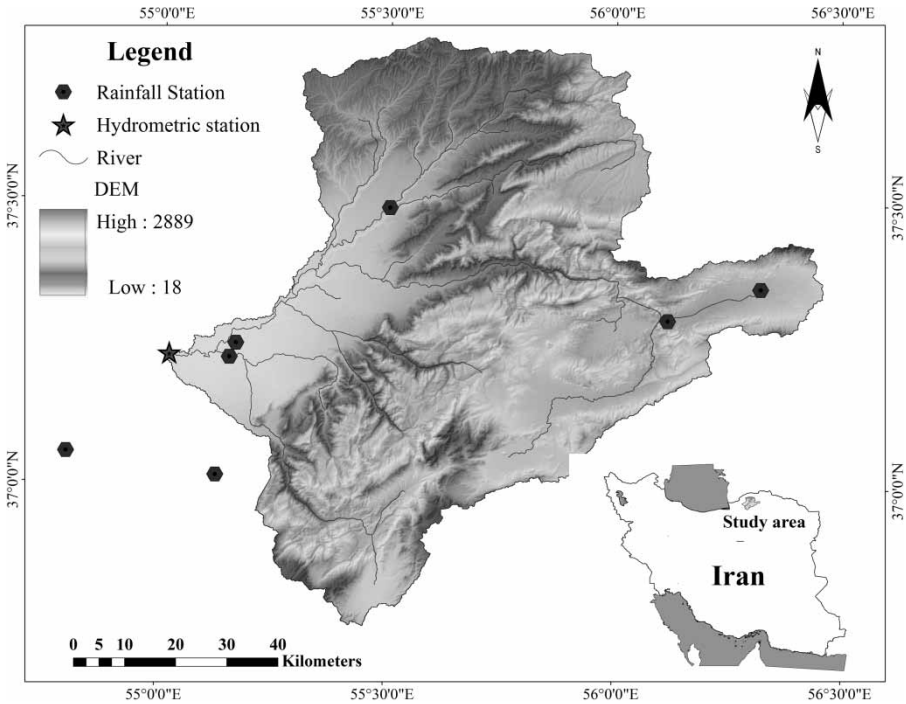

Figure 1 | Digital elevation map of the study area with major rivers and gauging stations.

The topographic maps came from the HydroSHEDS database, which is a mapping product based on NASA's 90 meter SRTM (Shuttle Radar Topography Mission) data. The soil data were built from the Food and Agriculture Organization (FAO) of the United Nations and 1:250,000 soil map of the Soil and Water Research Institute of Iran. The detailed soil properties (i.e., texture, water content, hydraulic conductivity, bulk density, clay content, silt, and sand) were obtained from available soil samples through the Natural Resources and Watershed Management Organization of Golestan province, Iran. A land use/cover map was produced based on Landsat TM image in the year 1997 with a spatial resolution of 30 m. The locations and details of rainfall and temperature stations are shown in Figure 1 and Table 1, respectively.

Hydrological model

SWAT is a basin-scale model designed to simulate watershed and water-quality processes, simulating the entire hydrologic cycle, including surface runoff, snowmelt, lateral soil flow, ET, infiltration, deep percolation, and groundwater return flows. It has previously been applied in Iran and has given satisfactory results (Salmani *et al.* 2012; Golshan *et al.* 2015; Jafarzadeh *et al.* 2016a). For this study, surface runoff was estimated using the Soil Conservation Service's Curve Number method, which is a nonlinear function of precipitation and retention coefficient. The Muskingum routing procedure was selected for routing the channel flow. Any water that does not become surface runoff enters the soil column. Soil-water can be removed by ET, deep percolation into the deep aquifer, or move laterally in the soil column for streamflow contribution (Neitsch *et al.* 2005). In SWAT, a deep aquifer is a confined aquifer and is assumed to contribute to streamflow outside of the watershed of interest. Groundwater contribution to streamflow can be generated from shallow and deep aquifers and is based on the groundwater balance. Here, we used the Penman–Monteith method to calculate the potential evapotranspiration which simulates the hydrological cycle with a different time step by disaggregating a river basin into sub-basins and hydrologic response units (HRUs). HRUs are lumped land areas within the sub-basin that comprise unique land cover, soil, slope, and management combinations. An assumption is made that there is no interaction between HRUs within a single sub-basin. Loading from each HRU are calculated separately and then summed together to determine the total loadings from the sub-basin (Neitsch *et al.* 2005). The model parameters were estimated by the automatic calibration procedure with a monthly time step from 1983 to 1993, in which the period from 1984 to 1990 (5 years) was used for calibration and the period from 1991 to 1993 (3 years) for validation. Furthermore, the first two years observed runoff data prior to 1983 and were used as warm-up period to mitigate the influence of initial condition errors.

Table 1 | Characteristics of the rainfall and temperature stations

	Location			Annual observed (1983–1993)	
Station	Lat (°)	Long (°)	Elevation (ma.s.l)	Rainfall (mm)	T (°C)
ArazKoseh	37.22	55.15	35	452	18.3
Bahlekh	37.05	54.78	24	428	16.6
Chesmekhan	37.28	56.12	1,250	333	12.9
Ramiyan	37.02	55.13	200	886	16.3
RobatGarehbil	37.35	56.32	1,450	187	12.5
Gonbad	37.23	55.15	37	435	18.7
Tamar	37.48	55.50	132	508	18.2

Modeling approach

Long Ashton Research Station Weather Generator model (LARS-WG) incorporates predictions from 15 GCMs used in the IPCC Fourth Assessment Report (AR4) (Solomon *et al.* 2007). The GCM used in this study is MPEH5C developed at the Max-Planck Institute for Meteorology, Germany. The GCMs spatial resolution are too coarse to apply directly for impact assessment (Mearns *et al.* 2003), thus the future temperature and precipitation time series were obtained by applying statistically downscaled using the LARS-WG model. The data utilized in the form of daily time series for suitable climate variables are precipitation (mm), maximum and minimum temperature (°C), and solar radiation ($MJ/m^2/day$) (Semenov & Barrow 2002).

The daily precipitation (P) and daily maximum and minimum temperature (Tmax and Tmin) were used as

input to SWAT from one downscaled climate model under three different scenarios of greenhouse gas emissions, including a medium greenhouse gas emission's scenario (A1B, GHG of 720 ppm stabilization in 2100), a low greenhouse gas emission's scenario (B1, GHG of 550 ppm stabilization in 2100) and the highest increase in the concentration of greenhouse gases (A2, GHG emissions are assumed to continue growing) to predict the impact of future climate change on hydrology, while the remaining data were supplied by the built-in weather generator. The downscaled rainfall data were subsequently used as input into the calibrated model for generating rainfall and runoff scenarios. The SWAT model was then run with the future climate data while assuming constant issues (i.e., current land use). However, we recognize that land cover changes resulting from climatic changes and other human activity may affect the hydrology of the basin in ways that are not considered here.

RESULTS AND DISCUSSION

Calibration of LARS-WG

The downscaled daily rainfall simulated by LARS-WG is shown in Table 2. The Nash–Sutcliffe efficiency (E_{NS}) as the ratio of residual variance to measured data variances (Nash & Sutcliffe 1970) and the root mean square error (RMSE), which measures the difference between values predicted by a model and the values actually observed from the environment that is being modeled, were used in this study to assess different results. The E_{NS} has values between $-\infty$ and 1 and represents the proportion of initial variance explained by the model with values equal to 1 indicating a perfect fit between observed and predicted data. In general, the model was able to capture the daily data series very well. In term of Tmax, Tmin, and P, LARS-WG was superior to downscale at the western station, as compared to the eastern station (Cheshmeh and RobatGarehbil). The reasons for the less accurate GCM performance in this region are likely, far from the central cell of the MPEH5 model, the effects of the local topography, and the model descriptions of physical processes, which have a major influence on the pattern of precipitation over the region.

The differences in average observed and simulated LARS-WG for monthly precipitation over the regions were between 1.5 and 23 mm/month while the RMSE and E_{NS} values were 4.10–13.02 and 0.77–0.87, respectively. As shown in Table 3, the RMSE and E_{NS} of Tmin ranged between 0.24 and 0.58 and 0.87 and 0.95, respectively. It shows that the model performs slightly better than Tmax, with the RMSE and E_{NS} of LARS-WG ranged between 0.52 and 0.98 and 0.85 and 0.96, respectively.

Precipitation predictions, however, have a larger degree of uncertainty than those for temperature since precipitation is highly variable in space and the relatively coarse GCM models cannot adequately capture this variability (Bader *et al.* 2008). Overall, the results showed that downscaling method well-reproduced the Tmax, Tmin, and P. Moreover, GCM simulations of P are much more problematic than those for temperature. The results presented in Table 2 indicate that the LARS-WG model shows appropriate prediction and thus it was chosen to assess the future climate change.

The result of the projected period for the scenarios in the gauging stations across the basin is presented in Figures 2

Table 2 | The performance of LARS-WG model outputs

	Tmax		Tmin		P	
Station	E_{NS}	RMSE	E_{NS}	RMSE	E_{NS}	RMSE
ArazKoseh	0.93	0.60	0.93	0.24	0.85	7.28
Bahlekeh	0.94	0.56	0.91	0.35	0.83	8.52
Tamar	0.91	0.52	0.90	0.50	0.83	9.74
Cheshmeh	0.87	0.98	0.88	0.46	0.77	7.06
Ramiyan	0.89	0.72	0.91	0.47	0.82	13.02
RobatGarehbil	0.85	0.76	0.87	0.58	0.80	4.10
Gonbad	0.96	0.97	0.95	0.42	0.87	6.44

Table 3 | Goodness of fit for daily stream flow simulations

Index	Calibration	Validation
E_{NS}	0.72	0.80
R^2	0.73	0.83
d	0.91	0.95
p	0.62	0.74

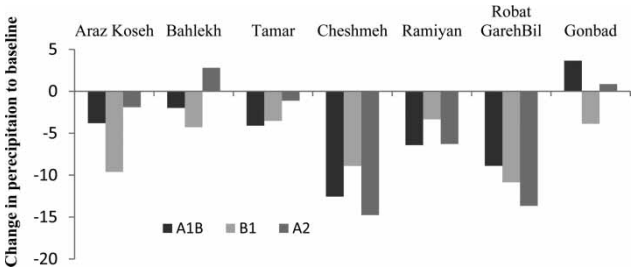

Figure 2 | Percentage changes in total annual precipitation relative to baseline for the three climate change scenarios at each gauging station.

and 3, in which the P, Tmin, and Tmax values for the 2020s were compared with the ones calculated for the outputs simulated under the baseline scenario (1980–2010) for each scenario.

The projected near-future changes in P are with different magnitudes and mostly indicating a decrease; however, a few stations also project increase of P, at Bahlekh gauging station (A2 = 2.79%) and Gonbad gauging station for A1B (3.64%) and A2 (0.86%) in respect to the baseline period (Figure 2).

Moving our attention to the mean annual P of the gauging stations trends of Figure 2, the A1 and A1B scenarios show a P decrease of 4.87%, whereas the scenario B1 shows a much greater P decrease of about 6.35% compared to the baseline period. Meanwhile the largest percentage changes in annual P are projected at Cheshmeh gauging station, which lies in the upper part of the basin, with a decrease mean annual P of 12.55, 8.90, and 14.76% under A1B, B1, and A2, respectively (Figure 2). The minimum change occurring at Gonbad gauging station is with a decrease in mean annual P of 3.87% under B1 scenario, and with an increase of 3.64 and 0.86% under scenario A1B and A2, respectively. The results indicate, compared to the period for which monitored records exist (1980–2010), a decrease of mean annual rainfall for the 2010–2030 period, with no significant indication of spatial variability of this decrease.

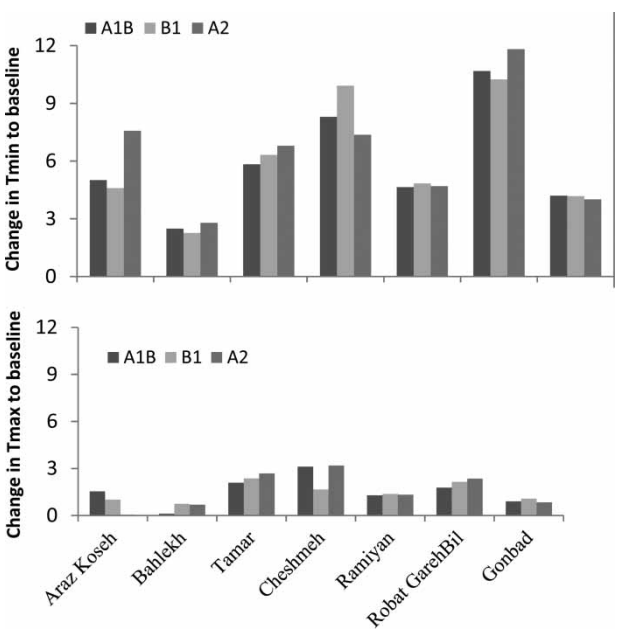

Figure 3 | The relative changes of annual Tmin and Tmax for the climate change scenarios with respect to the current conditions at each gauging station.

The projected scenarios in all gauging stations agree to an increment of Tmin between 2.26% and 11.82% in respect to the baseline period (Figure 3). The maximum relative changes in Tmin are projected to occur consistently at RobatGarehbil and Cheshmeh gauging stations.

The average Tmin projected by the model according to A2 scenario increases slightly more than the average Tmin in other scenarios (i.e., A1B and B1).

The variability changes for Tmax are generally moderate in all scenarios (Figure 3). All gauging stations reveal increases of Tmax for mid century in the basin, with 3.19% and 3.12% (Cheshmeh station) under the A2 scenario and A1B scenario, respectively, and 2.68% (Tamar station) under the A2 scenario. The magnitude of regional warming of Tmax in all scenarios at the gauging stations is close to each other.

Generally, the P changes vary substantially from month to month and across the basin in all scenarios. The percent change of P rate is generally greater on the eastern side of the GRB than the western side; conversely, the Tmin changes are mostly greater on the western side of the GRB than the eastern side, while Tmax variations over the basin did not follow a clear pattern.

The ensemble means of P, Tmin, and Tmax predictions with respect to the baseline period (1980–2010) under the MPEH5C, with A1B, B1, and A2 scenarios obtained from LARS-WG at seven gauging stations of the basin were calculated to further illustrate future change in the period of 2011–2030. Areal P, Tmax, and Tmin changes across the basin using Thiessen polygons were derived. The regionally

averaged percentage changes in monthly mean rainfall, Tmax, and Tmin in the 2020s with respect to the baseline period are presented in Figure 4. In the basin scale and under scenarios A1B, B1, and A2, the mean annual P is projected to decrease by 10.21%, 8.15%, and 8.83%, respectively. As shown in Figure 4, in the 2020s this may cause a decrease in monthly P in most months except in January, June, July, and August.

The highest rise in P was obtained by the A2 scenario in July (22.2%) followed by the B1 scenario in June (20.3%) and the highest reduction in P was obtained under A1B scenario in October by 26.2% followed by the A1 scenario (16.5%). P variability decreases in autumn and winter months (except for January) and increases in most of the summer months. Overall, seasonal mean of P is anticipated to decrease moderately in autumn, notably in September and October in the A1B scenario.

Figure 5 presents the resulting projections of regionally averaged Tmin and Tmax changes to the future climate. The GCM model indicates it is plausible that both Tmin and Tmax rise by less than 5% compared to the baseline over the GRB for all seasons, by the 2020s. For the 2020s, the A1B, B1, and A2 scenarios displayed annual Tmin increase by 3.4%, 3.0%, and 4.4%, respectively. Over the 2020s and compared to the past, Tmin increase reached +9.1% (April) for the A1B scenario and +10.3% (April) for the A2 scenario (Figure 5). The Tmin changes are predominantly positive in all months, except in the B1 scenario for March and November when increased winter temperatures will lead to potentially more rain than snow and melting starting earlier in the spring. An increase in mean monthly temperature during the summer months may significantly increase the evapotranspiration rates in the vegetated areas (Al-Mukhtar *et al.* 2014).

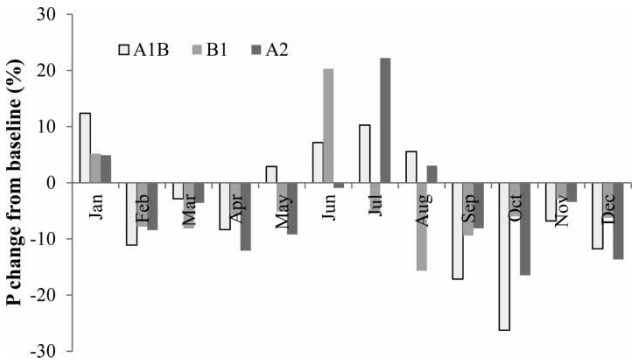

Figure 4 | Relative changes in monthly precipitation for A1B, B1, and A2 climate change scenarios with respect to the current condition.

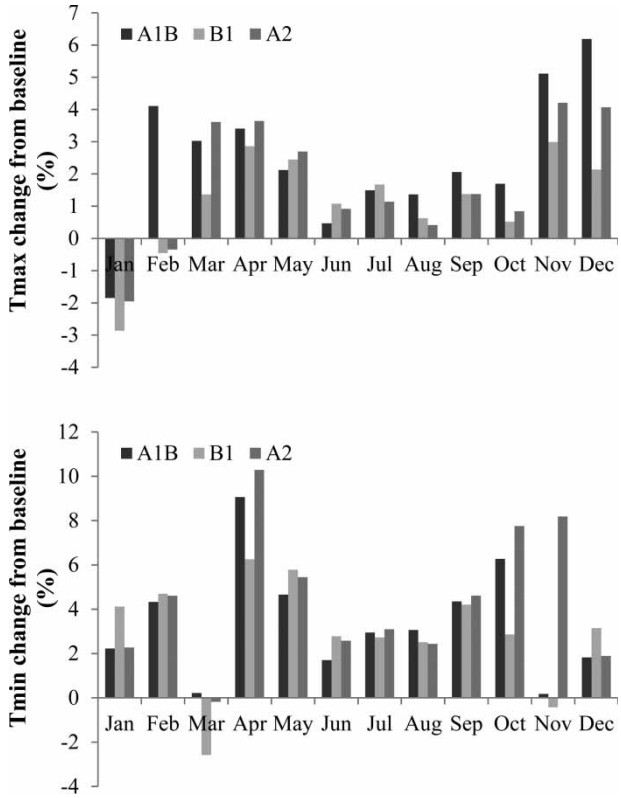

Figure 5 | The relative changes in monthly Tmax and Tmin for the climate change scenarios with respect to the current conditions.

The projected monthly Tmax scenarios of the catchment did not vary significantly under future scenarios (Figure 5), with mean increase of 1.7% to 2.7% in all scenarios. The Tmax showed an increase in mean monthly maximum temperature for all months except for January (Figure 5). The change in mean monthly Tmax ranged between −1.8% in January and +3.4% in April for the A1B scenario, between −2.8% in January and +3.0% in November for the B1 scenario, and between −1.9% in January and +4.21% in November for the A2 scenario. In general, the variability changes in the warmer months are relatively smaller than in the others. The mean monthly change in daily maximum temperature from the baseline period data would mean generally less variation of Tmax than Tmin and P.

Impact of climate change on stream flow

The informal generalized likelihood uncertainty estimation (GLUE) approach was used for uncertainty-based calibration of the SWAT model against the outlet gauge over the basin for 1983–1989 and validated for 1990–1993. Comparisons of the observed and simulated runoff of the SWAT model are shown in Figure 6. The peak values during the calibration period are generally underestimated while low flow discharge is relatively well simulated by the model. The efficiency values and visual inspection of hydrographs over the calibration period show that model performance is satisfactory. The Nash–Sutcliffe coefficient (E_{NS}) for streamflow was 0.72 and 0.80 for the calibration and validation periods, respectively. SWAT provided good performance in calibration on the objective functions while its validation performance was somewhat better compared to the calibration period with clearly reduced uncertainty bounds (Table 3). In the validation period, the predicted stream flow corresponded more closely to the measured flows, with less overprediction of peak flow months, as compared to the calibration period. SWAT simulated both wet and dry years reasonably, which subsequently can be used to evaluate the impact of climate change on stream flow (Figure 6). This implies that the model is successful in modeling the blue water flows in the GRB.

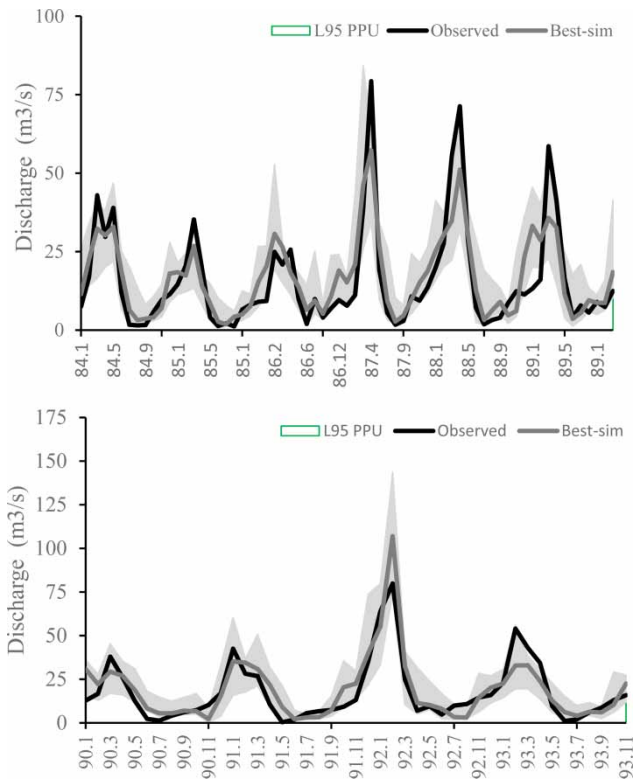

Figure 6 | Time series of the observed and simulated monthly stream flow data with 95% prediction uncertainty calculated by GLUE approach in calibration (left side) and validation (right side) periods at Gazaghly outlet.

Figure 7 illustrates the annual mean water balance (1984–1993) of the GRB at Gazaghly gauging station. It can be seen that the maximum rainfall was received in March (78.6 mm) and February (61.47 mm) and the lowest in July (15 mm) and June (18.7 mm), respectively. The highest overland flow resulted in March while the lowest was in July. The overland flow is generally higher in winter (104 mm) and autumn (63 mm) and lower in summer (25.5 mm) and spring (58 mm). Actual evapotranspiration at Gazaghly station shows a higher rate of evapotranspiration during spring and summer and a lower rate in autumn and winter, which is consistent with the changes in temperature, solar radiation, and growing season. Much of the runoff at Gazaghly is dominated by the quick flow contribution which accounts for an average of 67% of the total runoff, with values for individual months ranging from 2% in July to 17% in March. Mean quick flow was about two times higher than mean slow flow, increasing from five times in November to reduce by up to 50% in June.

The calculated air temperature and precipitation changes from a downscaled simulation of the future change (MPEH5C) with three different emission scenarios

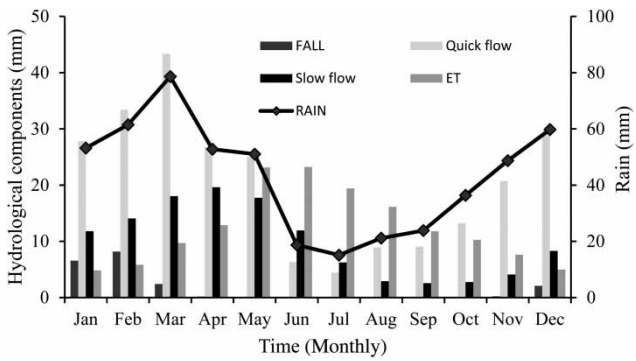

Figure 7 | The monthly water balance components in the GRB.

(SRES A1B, B2, and A1) was used to assess the future water balance changes in the GRB. All the other variables in SWAT remain constant; these three projections provided the input to the SWAT model to projected future climate changes. As seasonal patterns of water availability often differ from seasonal water needs, the seasonal distribution of decade-scale changes in precipitation, streamflow, and ET is as important as annual changes, which in turn may require management intervention to balance differences in water availability (Gabrecht *et al.* 2004). The results of climate change scenario simulations are representing 2010–2030 compared with the corresponding baseline period.

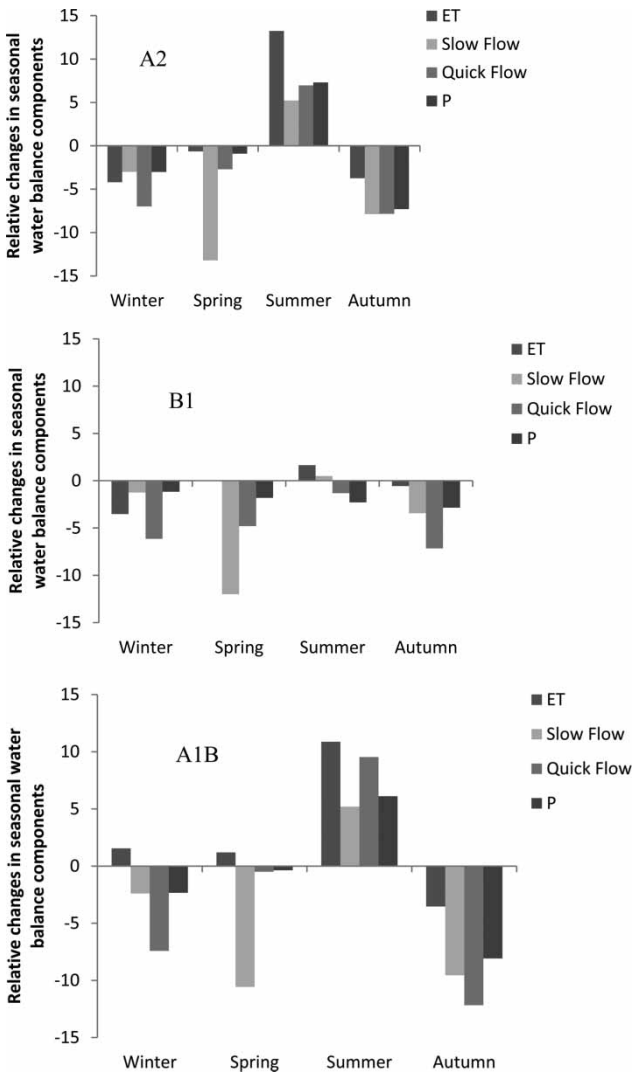

Figure 8 | Relative changes in seasonal water balance components: ET (■), slow flow (■), quick flow (■), and P (■) for the period 2020s in different scenarios.

Figure 8 shows the relative changes in water balance terms of the GRB predicted by SWAT, after temperature and precipitation were perturbed by SRES emission scenarios, for the 2020s.

The distribution of seasonal GCM projections in Figure 8 illustrates that the models were not in uniform agreement in the direction or magnitude of changes for the 2020s time period. The baseline period received the greatest contribution to seasonal P in the spring (March, April, May), followed by winter (December, January, February), autumn (September, October, November) and summer (June, July, August). This inter-seasonal behavior was maintained in all scenarios in the 2020s simulations. The projected winter, spring, and autumn climate resulted in a decrease of seasonal hydrological components relative to the baseline conditions for all scenarios, indicating that the projected decrease in precipitation exceeds the simulated decrease in evaporation. This is especially the case for A1B scenarios, which lead to a substantially lower simulated autumn quick flow. The relative decrease in quick flow and slow flow were always larger than the corresponding relative decrease in precipitation. In the 2020s, the quick flow by A1B and A2 scenarios in the summer compared to the baseline scenario were projected to increase by 9.5% and 7%, respectively. The most significant changes in quick flow were projected to occur in the autumn in all scenarios. However, the range of decrease is predicted to be between 12.6% (A1B), 13.2% (A2), and 13.3% (B1). It is noticed that seasonal slow flow consistently decreases over all seasons except for a slight increase in summer. In all modeled scenarios, the reduction of slow flow will be in the range of 1.25 to 13.9%, while it tends to increase in summer by 5.2%. However, quick flow increased more compared to the slow flow because the north and central parts of the basin have relatively flat topography. The projected winter P and winter slow flow have shown only a slight reduction in all scenarios. The largest decrease in seasonal slow flow will probably occur during the spring months with a decrease ranging from 10.6% to 13.9% which can be attributed to the decrease in average spring precipitation across the basin. The SWAT model predicts a higher summer slow flow in A2 scenario; in contrast, the slow flow trend results in a small (5%) but significant increase in ET by about 13%, from 58.7 mm to 66.5 mm in summer. This is likely

because of the feedback between precipitation and evapotranspiration via temperature also, on energy availability and surface wind. On the other hand, decreased ET in autumn in all scenarios reduced slow flow.

All of the modeled scenarios indicated an increase in ET in summer months; with respect to change in ET for GRB it is 0.5% for the B1 scenario, while the MPEH5C scenarios A1 and A1B show ET increase of 13.2% and 10.9%, respectively. ET from the near-future period 2010–2030 to the historic period 1980–2010 are greater for both A2 and A1B scenarios than for the B1 scenario in summer. The reduction in ET for the B1 scenario is 0.56%, which is less than that of the A1B (3.5%) and A2 (3.7%) scenarios.

Overall, the average quick flow and slow flow are projected to increase by 5 to 9% in summer in A2 and A1B scenarios due to the increased precipitation. These projections clearly rely on the uncertain changes in temperature and precipitation and might lead to increased flood risks with consequent impacts on soil erosion rate. The increased soil erosion would also clog the waterways and its channels by changing the river morphology, which would increase pollution and sedimentation by transporting pesticide, herbicides, and fertilizers from agricultural lands via the accelerated surface runoff. Water is important to plant growth, so varying precipitation patterns result in having impacts on crop productivity. As the GRB is dominated by rain-fed agriculture, the projection of future hydrological component changes can therefore be expected to impact on the magnitude and direction of climate impacts on crop production.

SUMMARY AND CONCLUSION

Analysis of the impact of climate change on water balance components was conducted by assessing the stream flow components simulated by SWAT using projected climate data for the historical (1983–1993) and projected (2020s) period based on a GCM model (MPEH5C) for three selected emissions scenarios in the GRB located in northeastern Iran. The LARS-WG model is used as a downscaling technique to generate the future temperature and precipitation which indicated that the annual precipitation will likely expect to decrease by about 3.5% in A1B and A2 scenarios with greater decreases for B1 scenario as compared to A1B and A2 scenarios. Moreover, the trends of P predicted for scenarios showed a similar seasonality change with a decrease in winter (A1B = 2.3%, B1 = 1.16%, and A2 = 3.0), autumn (A1B = 2.8%, B1 = 8.1%, and A2 = 7.3%) and slightly in spring in all scenarios while it is projected to increase in summer for all scenarios. As the largest rain-fed wheat area is cropped during the autumn season followed by a spring cropping, such changes may negatively affect the rain-fed agricultural sector. The largest decrease in monthly P can be observed in August (15.9%), September (15%), and October (11.75%) according to scenarios B1, A1B, and A2, respectively.

Although the magnitude of the changes not only varies by station, but also between scenarios, the overall pattern of the changes based on emission scenarios is obvious. In scenario A1B (A2), the largest decrease in annual P is likely to occur at Cheshmeh station, 12.55% (14.8%), followed by RobatGraehbil station, 8.9% (13.7%). The greatest decrease in precipitation in scenario B1 is predicted to occur at RobatGraehBil, 10.9%, followed by ArazKoseh, 9.6%.

The observed temperature across the GRB is projected to increase in all seasons, with a relatively greater increase in Tmin as compared to Tmax. The downscaling indicates an annual Tmax increase for the 2020s, but the variability is not significant. The largest increase in monthly Tmax in scenario A2 (B1) can be observed in November, 4.2% (3.0%). For scenario A1B, the increase in the Tmax is slightly higher than that for scenarios A2 and B1, while the projected Tmax is higher by 6.2% than the baseline in December.

In the basin scale, the downscaling indicates an annual Tmin increase for the 2020s by 4.5% (A2 scenario), 3.5% (B1 scenario), and 3.4% (A1B scenario). The seasonal Tmin is also expected to rise, but at different rates than the annual average. Projections based on SRES scenarios for spring (4.9%) and autumn (4.32%) are greater than those projected for winter (3.2%) and summer (2.6%). The expected Tmin could decrease slightly in March compared to the other months in A2 and B1 scenarios. Looking to scenario A1B (B1), the largest increase was in April (April), where the largest and smallest increases were 9.1% and 0.2% (6.2% and 2.5%), respectively, which is particularly strong for A2

scenario. Projected changes in Tmin are 3.4% (0.17% to 9.1%) by the A1B scenario, 3.5% (−2.6% to 6.2%) by the B1 scenario, and 4.4% (−0.18% to 10.3%) by the A2 scenario. Greater Tmin increases are projected for Cheshmeh station (>10%) for all scenarios, whereas Bahlekeh shows the lowest increase (<4%) for A1B and B2 scenarios.

Based on the temperature increases and precipitation decreases, climate change has the potential to modify streamflow regime and may result in a reduced streamflow by 6.02%, 5.2%, and 4.7% in B1, A2, and A1B scenarios in the coming decades, respectively, compared to the base period.

A rather insignificant change in the patterns of the components flow, which are derived from the three scenarios in question, may take place in the first 20 years of the century. At seasonal scale, average quick flow under the B1, A1B, and A2 scenarios is projected to decrease during autumn (7.2%–12.2%) and winter between 6.15% and 7.4% with no significant change in the summer and autumn months. Seasonal average slow flow under the emissions scenarios is projected to decrease by 1.25% to 13.2% with the largest declines according to A2 scenario, except for the summer where a slight increase is projected. Changes in intra-annual (monthly) components flow are greater and the greatest monthly increases of up to 29.4% and 12.2% are projected in June in quick flow and slow flow, respectively, and the greatest monthly decrease of up to 20% (August) is expected in the 2020s under B1 scenario compared to the base period. Under A1B scenario, the increase in quick flow and slow flow is pronounced in June (26.8%) and July (9.7%) while the decrease is more pronounced in October (21.8%) and September (17.6%), respectively. Quick flow is reduced up to 20.9% in October and increased by 25.2% in July in the A2 scenario and for slow flow the largest increases (15.2%) are projected in July while A2 scenario simulation projected the largest declines in October (13.2%). Increase in quick flow is observed for months which correspond to the increase in monthly P. The results indicated that by the 2020s the climate over the GRB will likely tend to towards substantial changes which may have widespread impacts on humans and the environment. However, we believe that our study has certain limitations. First, the present research assumed that future green and blue water flows solely result from meteorological changes and we neglected the joint impact of climate and land use changes on water balance. Second, the GBR is witnessing intense ongoing water resources management activities, e.g., dam construction, water consumption limitations per well, and closing of wells. Thus, simulations of future discharge do not include the operation policies. Furthermore, in the present analysis, we considered only one GCM from IPCC-AR4 and one hydrological model although three emission scenarios were included. Recent work highlights that there is uncertainty across different GCMs in the simulation of runoff (Lee & Kim 2017), therefore it cannot be assumed that all GHMs will perform in the same way as the GSM presented here. Lastly, our approach does not account for all sources of uncertainty involved with projecting future climate. The uncertainties of using different hydrological models and downscaling methods should be investigated to provide a useful guideline for evaluating the uncertainties in studies of climate change impacts on hydrology. This limitation should also be assessed in future developments of this study.

CONFLICT OF INTEREST

There is no conflict of interest.

REFERENCES

Al-Mukhtar, A., Dunger, V. & Mekel, B. 2014 Assessing the impacts of climate change on hydrology of the Upper Reach of the Spree River: Germany. *Water Resour. Manage.* **28**, 2731–2749.

Araghinejad, Sh., Shafaei, A. H. & MassahBavani, A. R. 2013 Assessment of climate change impacts on operation of Gorganrood basin's dams. *Water Irrig. Manage.* **3** (2), 43–58 (in Persian).

Arnell, N. W. 1992 Factors controlling the effects of climate change on river flow regimes in a humid temperature environment. *J. Hydrol.* **132** (1–4), 321–342.

Arnell, N. W. 2004 Climate change and global water resources: SRES emission and socio-economic scenarios. *Glob. Environ. Change* **14**, 31–52.

Bader, D., Covey, C., Gutkowski, W., Held, I., Kunkel, K., Miller, R., Tokmakian, R. & Zhang, M. 2008 *Climate Models: An Assessment of Strengths and Limitations. U.S. Climate Change Science Program Synthesis and Assessment Product*

3.1. Department of Energy, Office of Biological and Environmental Research, p. 124.

Delgado, J., Barba-Brioso, C., Nieto, J. & Boski, T. 2011 Speciation and ecological risk of toxic elements in estuarine sediments affected by multiple anthropogenic contributions (Guadiana saltmarshes, SW Iberian Peninsula): I. Surficial sediments. *Sci. Total Environ.* **409**, 3666–3679.

Gabrecht, J., Van Liew, M. & Brown, G. O. 2004 Trends in precipitation, streamflow, and evapotranspiration in the great plains of the United States. *J. Hydrol. Eng.* **9** (5), 360–367.

Ghorbani, K., Zakerinia, M. & Hezarjaribi, A. 2013 The effect of climate changes on water requirement of soybean in Gorgan. *J. Agric. Meteorol.* **2** (1), 60–72 (in Persian).

Golshan, M., Kaviyan, A., Rouhani, H. & Esmaili Ori, A. 2015 Multi-site calibration of runoff in Haraz watershed using SWAT model. *Iranian Journal of Soil and Water Research* **46** (2), 293–303 (in Persian).

Hatfield, J. L., Boote, K. J., Kimball, B. A., Ziska, L. H., Izaurralde, R. C., Ort, D., Thomson, A. M. & Wolfe, D. 2011 Climate impacts on agriculture: implications for crop production. *Agron. J.* **103**, 351–370.

Jafarzadeh, M. S., Rouhani, H., Salmani, H. & Fathabadi, A. 2016a Reducing uncertainty in a semi distributed hydrological modeling within the GLUE framework. *Journal of Water and Soil Conservation* **23** (1), 83–100 (in Persian).

Jafarzadeh, M. S., Rouhani, H., Heshmatpure, A. & Kashani, M. 2016b Detecting trend of meteorological series across the Gorganrood Basin in recent three decades. *J. Watershed Manage. Res.* **7** (13), 230–240 (in Persian).

Jiang, T., Chen, Y. D., Xu, C., Chen, X. & Singh, V. P. 2007 Comparison of hydrological impacts of climate change simulated by six hydrological models in the Dongjiang Basin, South China. *J. Hydrol.* **336**, 316–333.

Lal, P., Alavalpati, J. & Mercer, E. 2011 Socio-economic impacts of climate change on rural United States. *Mitig. Adapt. Strateg. Global. Change* **16** (7), 819–844.

Lee, J. K. & Kim, Y. O. 2017 Selection of representative GCM scenarios preserving uncertainties. *J. Water Climate Change*. DOI: 10.2166/wcc.2017.101.

Malekian, A. & Kazemzadeh, M. 2016 Spatio-temporal analysis of regional trends and shift changes of autocorrelated temperature series in Urmia Lake Basin. *Water Resour. Manage.* **30** (2), 785–803.

Mearns, L., Giorgi, F., Whetton, P., Pabon, D. & Hulme, M. 2003 *Guidelines for use of Climate Scenarios Developed From Regional Climate Model Experiments. Intergovernmental Panel on Climate Change Task Group on Data and Scenario Support for Impact and Climate Assessment (TGICA)*.

Modaresi, F., Araghinejad, Sh., Ebrahimi, K. & Kholghi, M. 2012 Assessment of climate change effects on the annual water yield of rivers: a case study of Gorganrood River, Iran. *J. Water Soil* **25** (6), 1365–1377 (in Persian).

Nash, J. E. & Sutcliffe, J. V. 1970 River flow forecasting through conceptual models, part I – a discussion of principles. *J. Hydrol.* **10**, 282–290.

Nearing, M. A., Pruski, F. F. & O'Neal, M. R. 2004 Expected climate change impacts on soil erosion rates: a review. conservation implications of climate change. *J. Soil Water Conserv.* **59** (1), 43–50.

Neitsch, S. L., Arnold, J. G., Kiniry, J. R., Williams, J. R. & King, K. W. 2005 *Soil and Water Assessment Tool Theoretical Documentation: Version 2005*. Texas Water Resources Institute, College Station, TX.

Parry, M. L., Canziani, O. F., Palutikof, J. P., van der Linden, P. J. & Hanson, C. E. 2007 *Climate Change: Impacts, Adaptation and Vulnerability. Contribution of Working Group II to the Fourth Assessment Report of the Intergovernmental Panel on Climate Change*. Cambridge University Press, Cambridge, UK.

Pasandidehfard, Z., Salman Mahini, A., Mirkarimi, S. H., Akbari, M. & Gholamalifard, M. 2014 Non-point source pollution modeling using geographic information system (GIS) for representing best management practices (BMP) in the Gorganrood Watershed. *Iranian J. Appl. Ecol.* **3** (8), 43–54 (in Persian).

Salmani, H., Mohseni Saravi, M., Rouhani, H. & Salajeghe, A. 2012 Evaluation of land use change and its impact on the hydrological process in the Ghazaghli Watershed, Golestan province. *J. Watershed Manage. Res.* **3** (6), 43–60 (in Persian).

Salmani, H., Mohseni Saravi, M., Rouhani, H. & Salajeghe, A. 2013 Evaluation of the efficiency of ArcSWAT model and ParaSOl software in runoff simulation (Case study: Ghazaghli Watershed, Golestan province). *Iran Watershed Manage. Sci. Eng.* **7** (22), 1–14.

Scanlon, T. S., Caylor, K. K., Levin, S. A. & Rodriguez-Iturbe, I. 2007 Positive feedbacks promote power-law clustering of Kalahari vegetation. *Nature* **449**, 209–212.

Schneeberger, K., Dobler, C., Huttenlau, M. & Stotter, J. 2015 Assessing potential climate change impacts on the seasonality of runoff in an Alpine watershed. *J. Water Climate Change* **6** (2), 263–277.

Semenov, M. A. & Barrow, E. M. 2002 LARS-WG: a stochastic weather generator for use in climate impact studies (Version 3.0). http://www.rothamsted.bbsrc.ac.uk/mas-models/larswg.html (accessed 26 March 2013).

Sheikh, V., Babaei, A. & Mooshakhian, Y. 2009 Trend analysis of precipitation regime in the Gorganroud Basin. *Iran Watershed Manage. Sci. Eng.* **3** (8), 29–38 (in Persian).

Shrestha, B., Babel, M. S., Maskey, S., van Griensven, A., Uhlenbrook, S., Green, A. & Akkharath, I. 2013 Impact of climate change on sediment yield in the Mekong River basin: a case study of the Nam Ou basin, Lao PDR. *Hydrol. Earth Syst. Sci.* **17**, 1–20.

Solomon, S., Qin, D., Manning, M., Marquis, M., Averyt, K. B., Tignor, M. & Miller, H. L. (eds) 2007 *Climate Change 2007: The Physical Science Basis. Contribution of Working Group I to the Fourth Assessment Report of the Intergovernmental*

Panel on Climate Change. Cambridge University Press, Cambridge.

Srikanthan, R. & McMahon, T. A. 2001 Stochastic generation of annual, monthly and daily climate data: a review. *Hydrol. Earth Syst. Sci.* **5** (4), 653–670.

Xu, C. Y. & Singh, V. P. 2004 Review on regional water resources assessment models under stationary and changing climate. *Water Resour. Manage.* **18**, 591–612.

Zang, C., Liu, J., van der Velde, M. & Fraxner, F. 2012 Assessment of spatial and temporal patterns of green and blue water flows under natural conditions in inland river basins in northwest China. *Hydrol. Earth Syst. Sci.* **16** (8), 2859–2870.

Zang, C., Liu, J., Gerten, D. & Jiang, L. 2015 Influence of human activities and climate variability on green and blue water provision in the Heihe River Basin, NW China. *J. Water Climate Change* **6** (4), 800–815.

First received 8 August 2015; accepted in revised form 12 October 2017. Available online 8 November 2017